STATISTICS, OPTIMIZATION AND INFORMATION COMPUTING
Stat., Optim. Inf. Comput., Vol. **15**, February 2026, pp 1195–1205.
Published online in International Academic Press (www.IAPress.org)

Autoencoder-Based Reconstruction and Restoration of 3D Dental Objects

Hamza MOUNCIF[1,*], Elmehdi ANIQ[2,3], Amine KASSIMI[1], Chaymae BENHAMMACHT[1]
Thierry Bertin GARDELLE[4], Mohamed CHAKRAOUI[2], Hamid TAIRI[1], Jamal RIFFI[1]

[1]*LISAC Laboratory, Department of Informatics, Faculty of Sciences Dhar El Mahraz, Sidi Mohamed Ben Abdellah University, Fez, Morocco*
[2]*LS2ME, Polydisciplinary Faculty of khouribga, Sultan Moulay Slimane University, Bénimellal, Morocco*
[3]*LAMIGEP, EMSI Marrakech, Marrakech Morocco*
[4]*3D Smart Factory, Mohamadia, Morocco*

Abstract This paper presents an exploration of autoencoders for 3D teeth reconstruction and completion, a crucial area in digital dentistry aimed at enhancing the efficiency of dental restoration and reconstruction. Accurate reconstruction of dental geometries is essential for developing personalized treatment plans and improving patient outcomes. However, most current approaches still rely on 2D imaging methods and often fall short of capturing the full complexity of tooth structures. In this study, we present a deep learning-based solution that effectively reconstructs 3D tooth models using point cloud representations. The results show that our method improve the accuracy of 3D tooth reconstruction and completion, as demonstrated by the results presented in these experiments. Our results have advancing digital dentistry techniques by providing a new methodology to utilize modern machine learning capabilities to enhance dental model reconstruction, which could lead to better treatment options, including the restorative treatments and the fabrication of customized dental prosthetics.

Keywords Point cloud, 3D tooth restoration, 3D tooth completion, auto-encoders, deep learning.

AMS 2010 subject classifications 68U10, 65D18

DOI: 10.19139/soic-2310-5070-2614

1. Introduction

Digital dentistry necessitates precise reconstruction and completion of 3D tooth models to be effective in the many applications it covers, including dental diagnostics, treatment planning, and production of dental prosthetics [30] . Traditional techniques generally employ 2D imaging techniques [15, 20], and do not represent the full three-dimensional complexity of the tooth structure as they are bound inherently constrained by 2D information available to them. However, with increased access to 3D scanning technology, paired with the growth of interest in point cloud data processing, we are beginning to see new avenues towards building accuracy and precision into the reconstruction of dental anatomy.
Autoencoders, a special type of neural network, known to learn efficient representations of data have gained popularity in a variety of domains, especially computer vision and medical imaging. Autoencoders encode input data in to latent space that is compact, and are then capable of reconstructing the original data from the latent representation, autoencoders have demonstrated their potential in tasks such as image denoising [3], anomaly detection [6], and dimensionality reduction [5]. In the context of dentistry, the application of autoencoders to

*Correspondence to: Hamza MOUNCIF (Email: Hamza.mouncif@usmba.ac.ma). LISAC Laboratory, Department of Informatics, Faculty of Sciences Dhar El Mahraz. Fez, Morocco (30050).

ISSN 2310-5070 (online) ISSN 2311-004X (print)

3D point cloud data holds the promise of revolutionizing the way tooth models are processed, analyzed, and reconstructed. In this research, we propose a novel approach for 3D point cloud tooth restoration and reconstruction using autoencoders.

The primary research problem addressed in this paper is the development of an efficient and accurate method for restoring and reconstructing a 3D tooth, leveraging the power of autoencoders. By focusing on point clouds as the input format, we aim to overcome the limitations of traditional 2D imaging techniques and provide a more comprehensive representation of tooth structures. Our proposed approach seeks to improve the fidelity of reconstructed models, ultimately enhancing the accuracy of dental diagnostics, and prosthetic design of 3D teeth. In summary, our work makes the following contributions:

- Direct 3D Reconstruction: We propose a method for reconstructing 3D teeth directly from point cloud data without intermediate 2D transformations.
- Significant Reduction in Reconstruction Time: Our approach reduces reconstruction time to under 1 second, compared to existing methods which can take up to 20 minutes.
- Evaluation on Clinical Dataset: We evaluate our model on a clinical dataset where it demonstrates strong performance both quantitatively, by minimizing reconstruction errors, and qualitatively, by preserving topological and surface details, outperforming current state-of-the-art techniques.

This paper is structured as follows: Section 2 provides a concise overview of current techniques for teeth reconstruction. Section 3 presents our proposed approach, detailing the architecture of the autoencoder model and the specific techniques employed in the encoder and decoder components. Section 4 describes the experimental setup, including the dataset used and the training procedure, also it includes a discussion about the results obtained from our experiments. Finally, Section 5 concludes the paper and outlines potential future research directions.

2. Related Works

Deep learning has made significant strides in dental healthcare, particularly in areas such as disease diagnosis and tooth segmentation [1, 2]. Networks employing deep learning techniques have proven highly effective, enhancing diagnostic accuracy [27, 18, 26, 28], and achieving superior results in tooth segmentation [16, 17, 19] .However, while deep learning methods have made strides in dental applications, the field of intelligent dental restoration is still emerging, a key limitation in existing deep learning-based teeth reconstruction approaches is that many do not operate directly on 3D objects, instead, they often apply dimensionality reduction or convert the objects to 2D images, which can hinder the precision and overall quality of the reconstruction result. For example Jon et al. [8] introduced an approach for modeling tooth shape variability using 3D scans of dental casts and Principal Component Analysis (PCA), they also employed regularization based on the differential geometrical properties of tooth surfaces to overcome the convergence issues of the log-likelihood estimator for small, high-dimensional datasets, this regularization acted as a Bayesian prior, enabling the reconstruction of missing teeth by identifying the most probable shapes that matches the tooth. Similarly Xu et al.[4] proposed a two-stage framework for reconstructing high-quality 3D objects of lower and upper teeth from intra-oral photographs. In the initial phase, they trained a diffusion model to generate multi-view consistent images and normal maps, this process was enhanced by a 3D-aware feature attention module, which helped maintain consistency between the different views. The second stage involved reconstructing 3D teeth models using geometry-aware neural implicit surface optimization based on the generated images and normal maps. While effective, the method has limitations, particularly in its time-consuming reconstruction process, which typically takes 10 to 20 minutes, additionally, the approach struggles with capturing finer details, as it does not capture low-level features with high-frequency information, limiting the overall precision of the reconstruction. Hwang et al. [15] proposed an approach for dental crown design that begins with creating 2D scan images of the opposing jaw, prepared jaw, and the gap distances from 3D intra-oral scans. These images are processed by a generative model to predict the best-fitting crown, based on expert designs. The used generative model follows the pix2pix [21] model, using a U-Net [22] generator with an encoder-decoder structure and symmetric skip connections. The generated 2D crown surface is then transformed back into a 3D object using CAD tools. Nevertheless, the approach is hampered by the time-consuming nature of

manual interaction and the dependence on CAD software.
Chafi et al. [9] introduced a method that utilizes a sphere of 2048 points as a global prior and a Gaussian distribution to create a prior latent matrix, establishing dense correspondence between the global prior and generated points through SP-GAN's part-editing and part-wise interpolation techniques [10], to enhance detailing, the generator incorporates graph attention modules connected to adaptive instance normalization, meanwhile, the discriminator uses a feature extraction module to classify shapes, determining if they are real or generated. Tian et al. [11] introduced a generative model that employs dilated convolutional layers to produce a feature map that maintains the distinct structure of dental tissues, additionally, their model employs a dual discriminator approach, which consists of two discriminators that work together to assess the input. The local discriminator focuses solely on the defective teeth to guarantee local consistency in the output, while the global discriminator evaluates the overall coherence of the generated dental crown by examining both the missing and adjacent teeth. Tian et al. [12] proposed a two-stage generative adversarial network (GAN) to reconstruct dental crown surfaces for restoring the masticatory function of broken teeth. In the first step a conditional GAN (CGAN) generates the basic occlusal surface shape, taking into account its spatial relationship with both the target crown and the impacted tooth. In the second step the occlusal surface is refined using an occlusal groove parsing network (GroNet) and occlusal fingerprint constraints to enhance its functional characteristics Similarly to Chau et al. [7] that employed a 3D Gan for reconstructing a 3D single-molar, Alexander et al. [13] proposed an approach for reconstructing occlusal surfaces using a two-step process. First, the 3D mesh data is normalized and projected into 2D space to effectively utilize the StyleGAN-2 [14] network. In the first step, StyleGAN-2 is trained with existing tooth morphology data, allowing it to generate a wide variety of occlusal surfaces, with the Adam optimizer used for both the generator and discriminator networks. In the second step, a Bayesian Image Reconstruction-based optimization process [23], leveraging the fixed generator from the fully trained StyleGAN-2 [14], reconstructs partial occlusal surfaces from the remaining tooth data .

3. Materials

3.1. Autoencoder

Autoencoders are a versatile neural network architecture designed to learn and extract representative features from data by encoding it into a lower-dimensional latent space and then reproducing the original input from the latent vector [31]. They are primarily used for unsupervised learning, where the goal is to capture the essential features of the input data while discarding noise or redundancies. This capability makes autoencoders highly valuable across a range of tasks, such as text summarization, restoring corrupted images, reconstructing missing parts in signals.
An autoencoder is composed of two primary components: the encoder and the decoder. The encoder compresses the input data $x \in \mathbb{R}^n$ into a lower-dimensional latent space $z \in \mathbb{R}^m$ $(where\ m < n)$, capturing the most relevant features while discarding irrelevant or redundant information. The decoder then reproduces the input data from this latent representation, the goal is to minimize the difference between the input data x and the reconstructed data $\hat{x}$, typically by minimizing the value of a loss function .
Accordingly, the model is trained through backpropagation with the weights of the encoder and the decoder both updated with the intention to minimize the error between the original data and the new reconstructed data. After several iterations, the autoencoder becomes effective and learns how to capture and reconstruct the the essential features of the input data.

3.2. 1D Convolutional Neural Network

Convolutional Neural Networks (CNNs) are a type of neural network specifically designed to handle Euclidean data with a grid-like topology, such as 2D images [32]. CNNs are widely used in image processing due to their ability to learn spatial hierarchies through the use of convolutional filters. In a 1D CNN, the convolution operation is applied to one-dimensional input data, making it an ideal tool for processing sequential data such as time series or flattened point clouds [25]. Unlike 2D convolutions used for image data, which slide filters across two dimensions (height

and width), 1D convolutions apply filters along a single dimension, capturing relationships between neighboring points or features in a sequence by applying equation 1.

$$\psi_v = b_v + \sum_{u=1}^{U} F_{v,u} \star \phi_u \tag{1}$$

Where:

- ψ_v is the output feature at position v,
- b_v is the bias term corresponding to position v,
- $F_{v,u}$ represents the convolutional filter applied at position u within the input sequence,
- $\star$ denotes the convolution operation,
- ϕ_u is the input feature at position u,
- U is the total number of input features in the sequence.

U represents the number of input channels and V represents the number of output channels, while d is the filter size. In a standard 1D convolutional layer, a vector of input features $\phi \in \mathbb{R}^{N\times U}$ is mapped to a vector of output features $\psi \in \mathbb{R}^{N\times V}$. The output features in the v-th channel are computed by convolving the filter $F_{v,u} \in \mathbb{R}^d$ with the input sequence $\phi_u \in \mathbb{R}^d$, and adding a bias term $b_v \in \mathbb{R}$. This convolution operation enables the network to effectively capture and encode local patterns and features within the input sequence.

3.3. MLP

The Multi-Layer Perceptron (MLP) is a foundational neural network architecture designed to model complex, non-linear relationships through its layered structure. At its core, the MLP consists of an input layer, several hidden layers, and an output layer, each contributing to its capability to model complex relationships. The input layer processes the raw data, which is then transformed through the hidden layers, while these hidden layers consist of neurons connected by weighted links and employ activation functions like ReLU or Sigmoid to introduce non-linearity, allowing the network to capture intricate patterns, then the output layer generates the final predictions, with its size corresponding to the output dimensions.
MLP networks are represented by a sequence of matrix multiplications and non-linear transformations, for an input vector $X \in \mathbf{R}^n$, where N is the number of input features, the network computes the output vector $Y \in \mathbf{R}^m$ through the following operation:

$$y_i = \sigma\left(\sum_{j=1}^{n_L} w_{ij}^{(L)} a_j^{(L-1)} + b_i^{(L)}\right) \tag{2}$$

Where y_i represents the predicted output for the i-th neuron in the output layer. The weight $w_{ij}^{(L)}$ connects the j-th neuron in the previous layer to the i-th neuron in the current output layer, and $b_i^{(L)}$ is the associated bias term. The activation function σ, such as ReLU or Sigmoid, is applied to the weighted sum to introduce non-linearity into the model. The term $a_j^{(L-1)}$ denotes the output of the j-th neuron in the previous layer. During training, the MLP adjusts its weights and biases to minimize the loss function(error), which measures the difference between the predicted outputs and the actual target values. This process involves calculating gradients using backpropagation and updating the parameters with optimization techniques like gradient descent.

4. Method

In this paper, we propose an innovative architecture for 3D point cloud tooth completion and reconstruction utilizing autoencoders Fig.1, specifically designed to handle point clouds , the proposed architecture takes 3D point cloud tooth as input,which is defined as a matrix of dimensions 4000x3 (4000 points, each point is presented on a 3D space x, y, z). Our proposed autoencoder different blocks as follow:

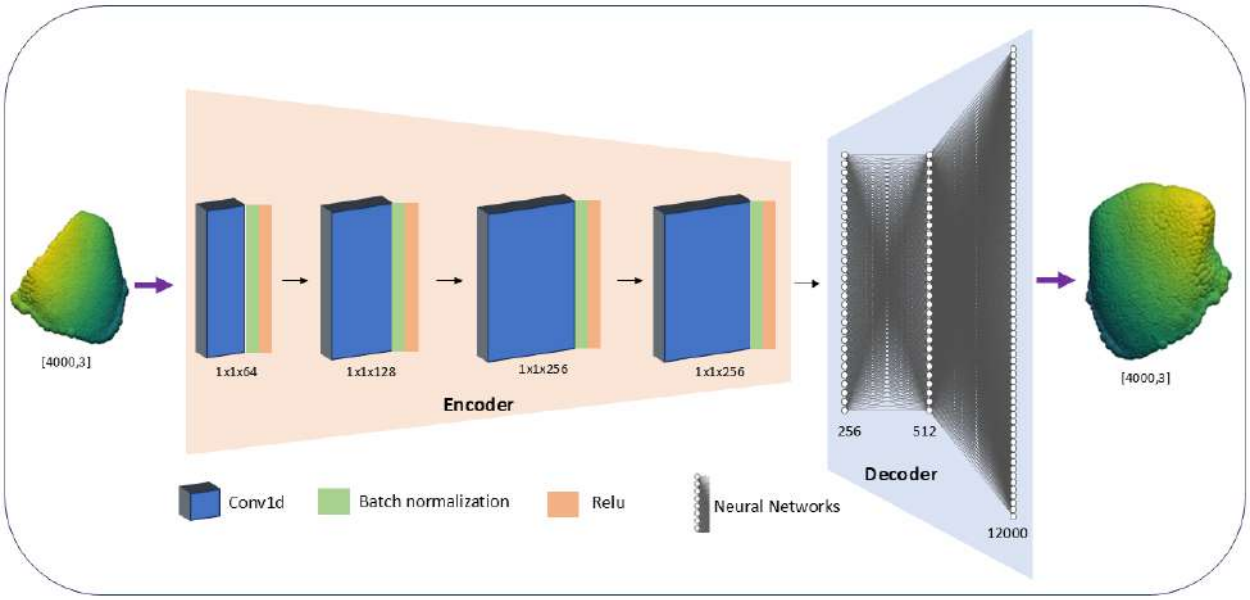

Figure 1. Our Proposed Autoencoder Architecture for 3D Point Cloud Tooth Reconstruction and Completion.

The encoder block employs a series of 1D convolutional layers (3.2), which systematically extract local features and capture hierarchical patterns from the input data, this layered architecture enables the model to progressively refine its understanding of the input, enhancing its ability to represent complex structures. The encoder is structured into four progressive 1D convolutional blocks, each designed to enhance feature extraction at increasing levels of abstraction. The first block applies 64 filters, the second 128 filters, followed by two blocks with 256 filters each. All filters have a kernel size of 1x1. Each convolutional layer is followed by batch normalization to accelerate and stabilize the training process. Similarly, every batch normalization is followed by a Rectified Linear Unit (ReLU) activation function, which introduces non-linearity and aids in capturing complex patterns within the data.
The decoder part converts the latent encoded vector back into a coherent 3D point cloud of the reconstructed teeth, the conversion is done through several dense layers which have a ReLU activation function after all neurons in those layers. The ReLU activation function provides non-linearity in the neural network structure and helps the model to learn more complex geometric details. The first layer consists of 256 neurons, followed by a second layer with 512 neurons, and the final layer comprises 12,000 neurons. This architecture is specifically designed to produce a detailed 3D representation of the teeth by effectively translating the intricate features learned by the encoder. After numerous training epochs, the decoder forms a point cloud that represents an accurate structure and form of the original teeth.

$$\begin{aligned} &\text{hausdorff}(P_1, P_2) = \frac{1}{2}\max_{x\in P_1}|x - \text{NN}(x, P_2)| + \frac{1}{2}\max_{x'\in P_2}|x' - \text{NN}(x', P_1)| \\ &\text{while } P_1 = \{x_i \in \mathbb{R}^3\}_{i=1}^{n} \;\&\; P_2 = \{x_j \in \mathbb{R}^3\}_{j=1}^{m} \\ &\text{and } \text{NN}(x, P) = \text{argmin}_{x'\in P}\|x - x'\| \textit{ is the nearest neighbor between two points} \end{aligned} \tag{3}$$

To evaluate the reconstruction quality, we utilized Hausdorff loss function (Eq.3). This loss metric quantifies the distance between the ground truth and the reconstructed point cloud, promoting a precise alignment of points and ensuring that the reconstructed model closely represents the original structure. By improving reconstruction fidelity, our method highlights the effectiveness of autoencoders in processing and completing 3D point cloud data, offering promising advancements for applications in diagnostic and treatment methodologies.

Our proposed architecture employs the Adam optimizer with a learning rate of 0.005, which effectively updates the weights and biases to minimize reconstruction and completion errors. It consisted of 200 epochs with a batch size of 100 to ensure efficient learning and convergence. The training process was performed on an NVIDIA Tesla P100 GPU with 16GB of VRAM, which provided the necessary computational power, and the entire training process took approximately four hours to complete.

5. Experiments

5.0.1. Dataset The dataset utilized in this study comprises raw maxillary teeth surfaces, directly acquired using the Medit intraoral scanner device. This dataset involved 28 individuals, resulting in 16 distinct tooth types, and yielding a total of 448 tooth objects, each tooth surface initially contained approximately 100,000 to 150,000 triangular faces. To facilitate processing while preserving the original topology, these surfaces were simplified to 7,500 triangular faces per tooth using the quadrilateral method [24]. Subsequently, they were converted to point clouds with 4,000 points by removing the edges connecting the vertices of the triangular faces. Figure 2 showcases examples from our dataset, providing a clear representation of the 3D teeth objects used in this study. The first row displays the teeth as triangular meshes, while the second row presents their corresponding point cloud conversions. Column A shows a molar tooth, Column B shows a premolar, and Columns C and D depict a canine and an incisor, respectively, illustrating the diversity of dental types in our study.
To safeguard participant privacy and confidentiality, all data were preprocessed and anonymized. We adhered to established ethical standards throughout the data collection, processing, and usage phases, ensuring compliance with research integrity and privacy regulations

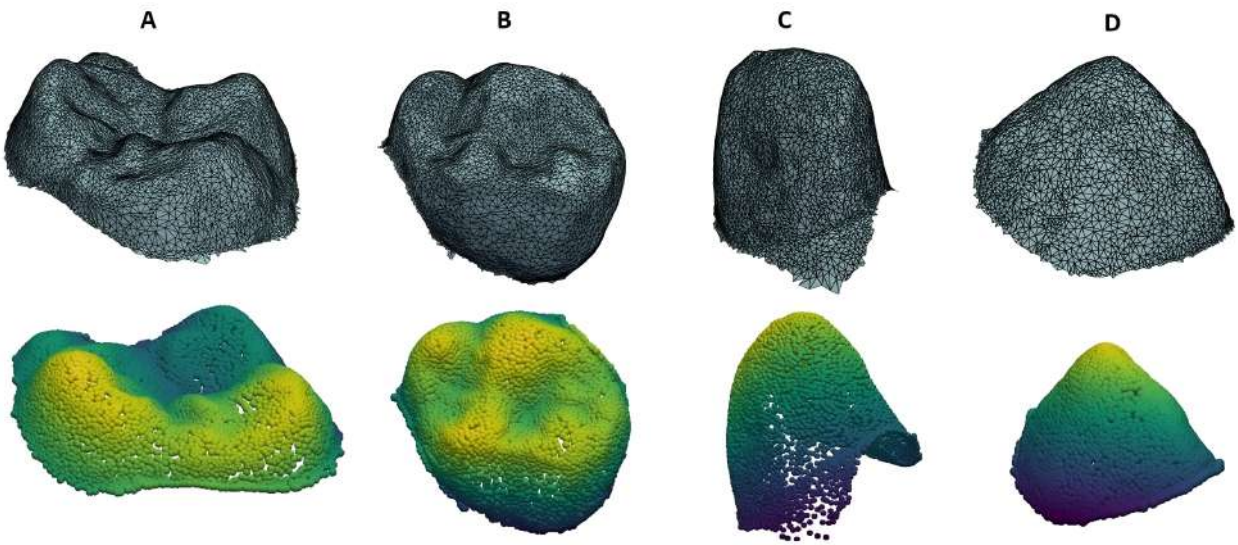

Figure 2. Examples of 3D Teeth in Our Dataset: The first row shows teeth represented as triangular meshes, while the second row displays the teeth converted to 3D point clouds, which are then fed into our architecture

$$P' = (R(\alpha).P^t)^t$$
$$\text{Where } R(\alpha) = \begin{bmatrix} \cos^2\alpha & \cos\alpha(\sin^2\alpha - \sin\alpha) & \cos^2\alpha\sin\alpha + \sin^2\alpha \\ \cos\alpha\sin\alpha & \sin^3\alpha + \cos^2\alpha & \cos\alpha(\sin^2\alpha - \sin\alpha) \\ -\sin\alpha & \sin\alpha\cos\alpha & \cos^2\alpha \end{bmatrix} \tag{4}$$

P^t is the original point cloud and $\boldsymbol{\alpha}$ is the rotation degree

To enhance the robustness and variability of the dataset, extensive data augmentation techniques were applied. Each tooth object was randomly rotated using equation 4 to simulate various natural orientations and positions. This process generated 20 additional variations for each original tooth object, significantly increasing the dataset's size and diversity. In total, the augmented dataset comprised 8,960 3D tooth objects. Subsequently, a normalization operation (Eq.5) was performed on each point $P_i = (x_i, y_i, z_i)$ in the 3D point cloud of each object to ensure uniformity in scale and orientation . This normalization aligns the point clouds to a standard coordinate system and rescaled them to a consistent size, a critical step for optimizing the training process of the neural network.

$$\mathbf{P}_i^{\text{normalized}} = \frac{\mathbf{P}_i - \mathbf{P}_{\text{mean}}}{\max\left(\|\mathbf{P}_i - \mathbf{P}_{\text{mean}}\|\right)}$$
$$Where:$$
- $\mathbf{P}_i$ is the original point in the point cloud.
- $\mathbf{P}_{\text{mean}} = \frac{1}{N}\sum_{i=1}^{N}\mathbf{P}_i = \left(\frac{1}{N}\sum_{i=1}^{N}x_i, \frac{1}{N}\sum_{i=1}^{N}y_i, \frac{1}{N}\sum_{i=1}^{N}z_i\right)$ is the mean of all points in the cloud.
- $\max(\|\mathbf{P}_i - \mathbf{P}_{\text{mean}}\|)$ is the maximum norm among all points.

(5)

For the training procedure, the dataset was randomly separated into testing and training datasets: 7160 tooth objects were assigned to training and 1800 tooth objects were assigned for testing the trained model.

5.0.2. Results Our 3D teeth reconstruction approach achieved minimal Hausdorff distance (HD) (Eq.3) and Chamfer distance (CD) values of **0.1978** and **0.0614**, respectively. The quantitative results indicate that our method outperforms current state-of-the-art approaches, as shown in Table 1.

Method	HD (mm)	CD (mm)
Xu et al [4]	2.1126	0.1670
Chau et al [7]	0.633	-
Chafi et al [9]	0.2213	-
Ours	**0.1978**	**0.0614**

Table 1. Quantitative results of our proposed architecture compared to the existing state-of-art methods.

One of the key advantages of our proposed approach is its ability to work directly with 3D teeth objects, unlike most existing methods that rely on 2D photographs. By focusing on 3D objects, this study offers a unique perspective in the field of dental reconstruction, providing a more comprehensive and accurate representation of the teeth, our proposed method has the potential to enhance the precision of dental treatments and improve patient outcomes. Our proposed autoencoder-based method demonstrates exceptional performance in generating accurate, high-quality dental models, making it as a valuable tool for both clinical and research applications. As shown in Fig.3, the qualitative evaluation compares reconstructed teeth to the input and original data. The model successfully captures the distinct geometrical features of different tooth types, ex: reproducing the canine (3, right part, C) is reproduced with sharp, smooth edges and subtle curvature, preserving its elongated form and well-defined crown.

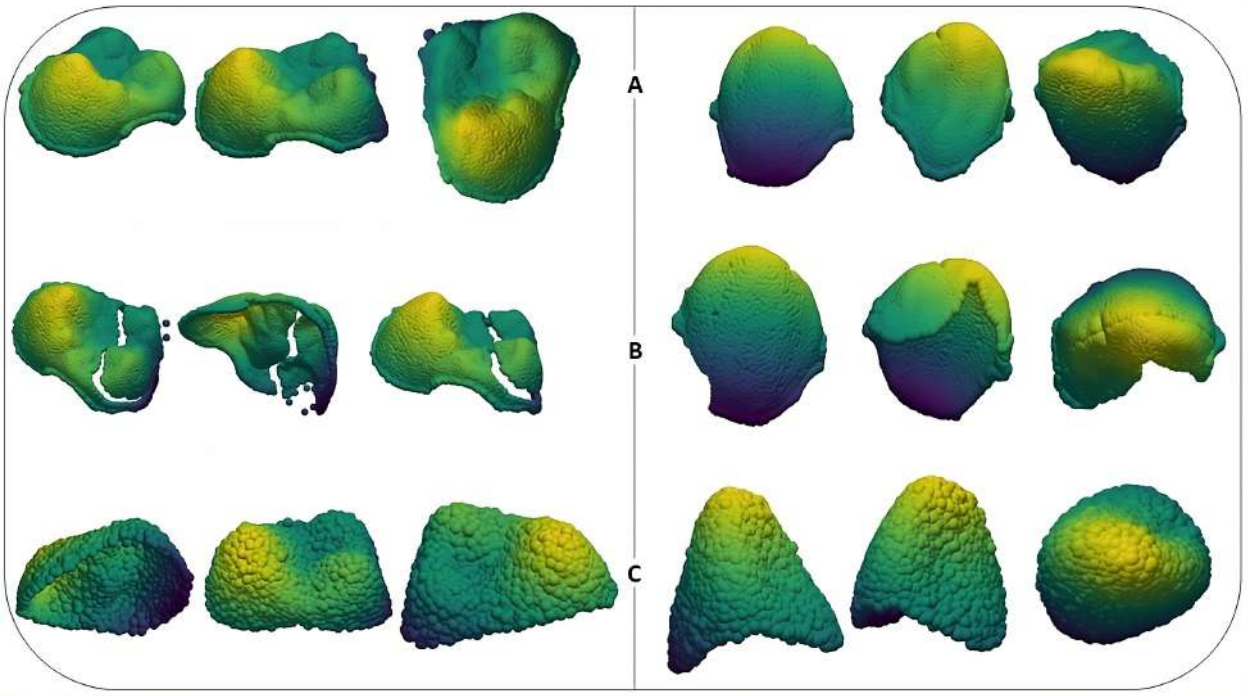

Figure 3. The first row of samples displays the input 3D dental models, while the row below shows our proposed approach's newly reconstructed objects. This arrangement highlights the accuracy and detail captured by the reconstructions.

Similarly, the 3rd molar (3, left part, C), with its more intricate, multi-faceted structure, including its wider, irregular crown and deeper grooves. The precise handling of these distinct shapes highlights the autoencoder's ability to generalize across different dental anatomies, a critical feature in achieving anatomically accurate reconstructions. The fine details, such as subtle curves and surface textures, are preserved in the reconstructions, illustrating the model's capacity to learn and reproduce intricate patterns inherent in dental structures. Moreover, to validate the smoothness and continuity of the reconstructed 3D tooth surfaces, we implemented an additional visualization by converting the 3D point cloud to a triangular mesh. Figure 4 presents different dental types following this conversion: The first part (Fig.4-(1)) shows a reconstructed canine tooth, which exhibits a robust and elongated crown, characterized by a prominent, well-defined cusp that tapers to a sharp point ((1), V3). The mesial and distal surfaces exhibit a slight convex curvature ((1), V1, V2), facilitating proper alignment with adjacent teeth. In the second part (Fig.4-(2)), a premolar is presented, where the occlusal table is slightly concave ((2), V2), allowing for optimal food processing. The model reproduces the smooth, rounded contour of the tooth ((2), V1), as well as the grooves between the cusps ((2), V3), indicating its ability to accurately reconstruct both the functional and aesthetic aspects of the premolar. In the last part (Fig.4-(3)), an incisor is shown, which is characterized by its smooth and flat surface ((3), V1). The model effectively captures the straight edges and the smooth tapering of the crown ((3), V3), as well as the labial surface, which is smooth and slightly convex ((3), V1), highlighting the model's capacity to handle simpler geometries while preserving surface smoothness. The model's ability to handle such complex and varied shapes showcases the autoencoder's robustness in generalizing across diverse dental anatomies, ensuring anatomically accurate reconstructions that faithfully reflect the intricacies of different tooth types, which reinforces the potential of our proposed approach to significantly advance the field of 3D teeth reconstruction.

Furthermore, our method excels in computational efficiency, it can reconstruct new 3D teeth object in less than **1 second**, making it highly suitable for real-time applications, such as chairside dental treatments. This is a substantial improvement over the method proposed by Xu et al. [4], which takes 10–20 minutes for a single

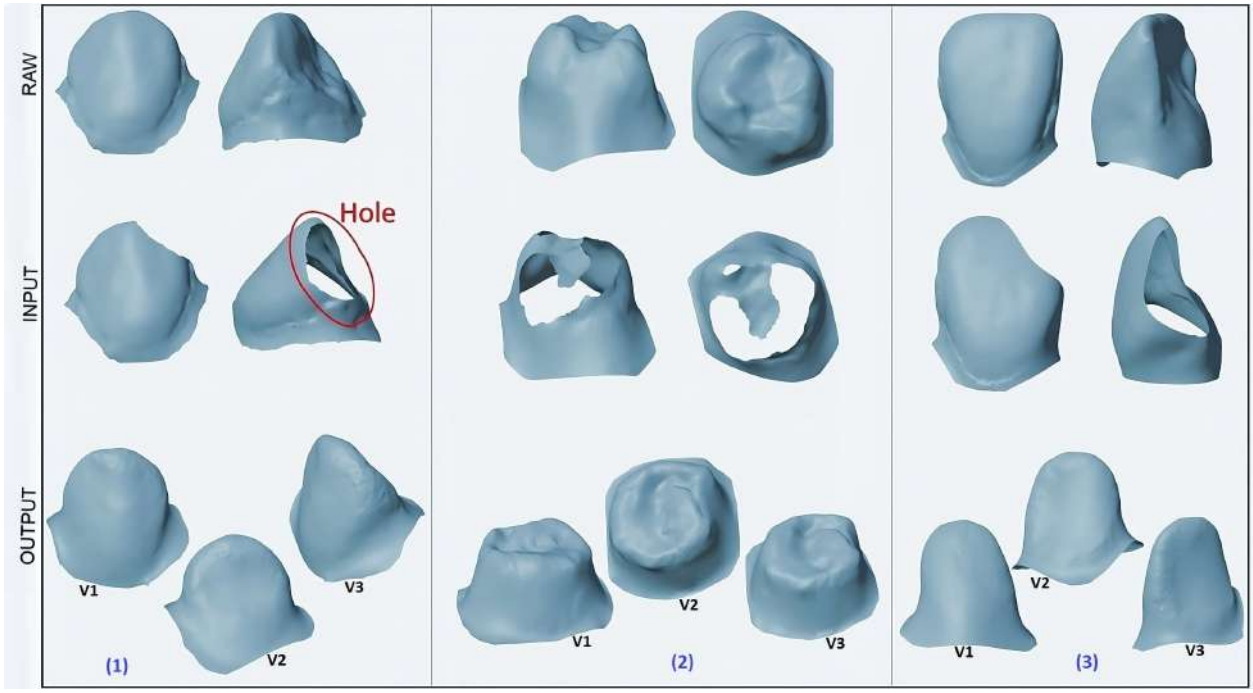

Figure 4. Example of original (1st row), input (2nd row), and reconstructed (3rd row) teeth of different dental types after point cloud conversion to 3D triangular mesh, illustrated in various angles.

reconstruction, making their approach impractical for time-sensitive environments, highlighting the substantial time savings offered by our approach. The superior accuracy of our method, combined with its speed, makes it a valuable tool not only for clinical and research purposes but also for practical use in dental diagnostics and prosthetic design.

Furthermore, we envision the integration of this method into clinical workflows, allowing for the automatic generation of accurate 3D dental models from patient scans. This could assist dental professionals in prosthesis design, treatment planning, and overall patient care. Through these efforts, we aim to contribute to the ongoing advancements in digital dentistry and improve patient outcomes. In future work, we also plan to evaluate the method's compatibility with existing CAD/CAM systems and assess its clinical effectiveness through practitioner-led case studies, enabling smoother adoption into real-world dental environments.

6. Discussion

In our effort to achieve high-quality 3D dental model reconstructions, we experimented with several methods before arriving at our proposed approach. One of the initial strategies involved using a Latent-GAN [33], which is known for its ability to generate and reconstruct realistic objects. Unfortunately this method didn't show satisfied results in the context of 3D tooth reconstruction, it produced results with a mean Hausdorff distance of **2.628**, which is significantly higher than the error achieved by our method. This result suggests that, despite their success in other domains, Latent-GANs struggle to capture the complex anatomical structure required for accurate 3D dental model reconstruction.

another method we explored consisted of an autoencoder with two recurrent neural network (RNN) [29] blocks in the encoder, and a multilayer perceptron network as the decoder. The intent was to leverage the sequential processing capabilities of RNNs to capture spatial dependencies within the point cloud data. However, this method

did not yield satisfactory results, achieving a mean Hausdorff distance of **1.672**. In comparison, our proposed method demonstrated superior performance.

7. Conclusion and Perspectives

This research demonstrates the effectiveness of employing autoencoders in 3D teeth reconstruction and completion, outperforming Latent-GANs and RNNs. Our method is capable of accurately reconstructing and completing complex dental geometries based on 3D point cloud input data. Nonetheless, a key limitation of the methodology lies in the high resolution 3D dental models which are resource-intensive to train therefore 3D dental models were simplified during preprocessing, potentially eliminating some anatomical details. In future work, we aim to address this challenge by focusing on leveraging the full complexity of 3D objects to capture more precise geometries and preserve anatomical structures, rather than relying on preprocessing simplification. Additionally, we plan to augment the dataset to include a wider variety of tooth shapes and conditions to improve the model's robustness and generalization. We will also refine the autoencoder architecture by exploring advanced techniques that could further improve the quality and accuracy of the reconstructions. Furthermore, we envision the integration of this method into clinical workflows, allowing for the automatic generation of accurate 3D dental models from patient scans. This could assist dental professionals in prosthesis design, treatment planning, and overall patient care. Through these efforts, we aim to contribute to the ongoing advancements in digital dentistry and improve patient outcomes. In future work, we also plan to evaluate the method's compatibility with existing CAD/CAM systems and assess its clinical effectiveness through practitioner-led case studies, enabling smoother adoption into real-world dental environments.

REFERENCES

1. Sivari, E., Senirkentli, G., Bostanci, E., Guzel, M., Acici, K. & Asuroglu, T. Deep learning in diagnosis of dental anomalies and diseases: A systematic review. *Diagnostics*. **13**, 2512 (2023)
2. Bayrakdar, I., Orhan, K., Akarsu, S., Çelik, Ö., Atasoy, S., Pekince, A., Yasa, Y., Bilgir, E., Sağlam, H., Aslan, A. & Others Deep-learning approach for caries detection and segmentation on dental bitewing radiographs. *Oral Radiology*. pp. 1-12 (2022)
3. Bajaj, K., Singh, D. & Ansari, M. Autoencoders based deep learner for image denoising. *Procedia Computer Science*. **171** pp. 1535-1541 (2020)
4. Xu, C., Liu, Z., Liu, Y., Dou, Y., Wu, J., Wang, J., Wang, M., Shen, D. & Cui, Z. TeethDreamer: 3D Teeth Reconstruction from Five Intra-oral Photographs. *ArXiv Preprint ArXiv:2407.11419*. (2024)
5. Boquet, G., Morell, A., Serrano, J. & Vicario, J. A variational autoencoder solution for road traffic forecasting systems: Missing data imputation, dimension reduction, model selection and anomaly detection. *Transportation Research Part C: Emerging Technologies*. **115** pp. 102622 (2020)
6. Zhou, C. & Paffenroth, R. Anomaly detection with robust deep autoencoders. *Proceedings Of The 23rd ACM SIGKDD International Conference On Knowledge Discovery And Data Mining*. pp. 665-674 (2017)
7. Chau, R., Hsung, R., McGrath, C., Pow, E. & Lam, W. Accuracy of artificial intelligence-designed single-molar dental prostheses: A feasibility study. *The Journal Of Prosthetic Dentistry*. **131**, 1111-1117 (2024)
8. Sporring, J. & Hommelhoff Jensen, K. Bayes reconstruction of missing teeth. *Journal Of Mathematical Imaging And Vision*. **31** pp. 245-254 (2008)
9. Chafi, I., Cheriet, F., Keren, J., Zhang, Y. & Guibault, F. 3D generation of dental crown bottoms using context learning. *Medical Imaging 2024: Imaging Informatics For Healthcare, Research, And Applications*. **12931** pp. 98-104 (2024)
10. Song, X., Chen, Y., Feng, Z., Hu, G., Yu, D. & Wu, X. SP-GAN: Self-growing and pruning generative adversarial networks. *IEEE Transactions On Neural Networks And Learning Systems*. **32**, 2458-2469 (2020)
11. Tian, S., Huang, R., Li, Z., Fiorenza, L., Dai, N., Sun, Y. & Ma, H. A dual discriminator adversarial learning approach for dental occlusal surface reconstruction. *Journal Of Healthcare Engineering*. **2022**, 1933617 (2022)
12. Tian, S., Wang, M., Dai, N., Ma, H., Li, L., Fiorenza, L., Sun, Y. & Li, Y. DCPR-GAN: dental crown prosthesis restoration using two-stage generative adversarial networks. *IEEE Journal Of Biomedical And Health Informatics*. **26**, 151-160 (2021)
13. Broll, A., Rosentritt, M., Schlegl, T. & Goldhacker, M. A data-driven approach for the partial reconstruction of individual human molar teeth using generative deep learning. *Frontiers In Artificial Intelligence*. **7** pp. 1339193 (2024)
14. Karras, T., Laine, S., Aittala, M., Hellsten, J., Lehtinen, J. & Aila, T. Analyzing and improving the image quality of stylegan. *Proceedings Of The IEEE/CVF Conference On Computer Vision And Pattern Recognition*. pp. 8110-8119 (2020)
15. Hwang, J., Azernikov, S., Efros, A. & Yu, S. Learning beyond human expertise with generative models for dental restorations. *ArXiv Preprint ArXiv:1804.00064*. (2018)
16. Cheng, B. & Wang, W. Dental hard tissue morphological segmentation with sparse representation-based classifier. *Medical & Biological Engineering & Computing*. **57** pp. 1629-1643 (2019)

17. Lian, C., Wang, L., Wu, T., Wang, F., Yap, P., Ko, C. & Shen, D. Deep multi-scale mesh feature learning for automated labeling of raw dental surfaces from 3D intraoral scanners. *IEEE Transactions On Medical Imaging*.
18. Mouncif, H., Kassimi, A., Bertin Gardelle, T., Tairi, H., & Riffi, J. (2025). 3D tooth identification for forensic dentistry using deep learning. *BMC Oral Health, 25*(1), 665. https://doi.org/10.1186/s12903-025-06017-y
19. Zhang, L., Zhao, Y., Meng, D., Cui, Z., Gao, C., Gao, X., Lian, C. & Shen, D. Tsgcnet: Discriminative geometric feature learning with two-stream graph convolutional network for 3d dental model segmentation. *Proceedings Of The IEEE/CVF Conference On Computer Vision And Pattern Recognition*. pp. 6699-6708 (2021)
20. Kokomoto, K., Okawa, R., Nakano, K. & Nozaki, K. Tooth development prediction using a generative machine learning approach. *IEEE Access*. (2024)
21. Henry, J., Natalie, T. & Madsen, D. Pix2pix gan for image-to-image translation. *Research Gate Publication*. pp. 1-5 (2021)
22. Ronneberger, O., Fischer, P. & Brox, T. U-net: Convolutional networks for biomedical image segmentation. *Medical Image Computing And Computer-assisted Intervention–MICCAI 2015: 18th International Conference, Munich, Germany, October 5-9, 2015, Proceedings, Part III 18*. pp. 234-241 (2015)
23. Marinescu, R., Moyer, D. & Golland, P. Bayesian image reconstruction using deep generative models. *ArXiv Preprint ArXiv:2012.04567*. (2020)
24. Daniels, J., Silva, C., Shepherd, J. & Cohen, E. Quadrilateral mesh simplification. *ACM Transactions On Graphics (TOG)*. **27**, 1-9 (2008)
25. Kassimi, A., Riffi, J., El Fazazy, K., Gardelle, T., Mouncif, H., Mahraz, M., Yahyaouy, A. & Tairi, H. 1D CNNs and face-based random walks: A powerful combination to enhance mesh understanding and 3D semantic segmentation. *Computer Aided Geometric Design*. **113** pp. 102379 (2024)
26. Liu, L., Xu, J., Huan, Y., Zou, Z., Yeh, S. & Zheng, L. A smart dental health-IoT platform based on intelligent hardware, deep learning, and mobile terminal. *IEEE Journal Of Biomedical And Health Informatics*. **24**, 898-906 (2019)
27. Wu, C., Tsai, W., Chen, Y., Liu, J. & Sun, Y. Model-based orthodontic assessments for dental panoramic radiographs. *IEEE Journal Of Biomedical And Health Informatics*. **22**, 545-551 (2017)
28. Lai, Y., Fan, F., Wu, Q., Ke, W., Liao, P., Deng, Z., Chen, H. & Zhang, Y. LCANet: learnable connected attention network for human identification using dental images. *IEEE Transactions On Medical Imaging*. **40**, 905-915 (2020)
29. Schmidt, R. Recurrent Neural Networks (RNNs): A gentle Introduction and Overview. *CoRR*. **abs/1912.05911** (2019), http://arxiv.org/abs/1912.05911
30. Broll, A., Goldhacker, M., Hahnel, S. & Rosentritt, M. Generative deep learning approaches for the design of dental restorations: A narrative review. *Journal Of Dentistry*. pp. 104988 (2024)
31. Bank, D., Koenigstein, N. & Giryes, R. Autoencoders. *CoRR*. **abs/2003.05991** (2020), https://arxiv.org/abs/2003.05991
32. O'Shea, K. & Nash, R. An Introduction to Convolutional Neural Networks. *CoRR*. **abs/1511.08458** (2015), http://arxiv.org/abs/1511.08458
33. Kalwar, S., Aich, A. & Dixit, T. LatentGAN Autoencoder: Learning Disentangled Latent Distribution. *ArXiv Preprint ArXiv:2204.02010*. (2022)